

Article

# Evaluation of a Simplified Method to Estimate the Peak Inter-Story Drift Ratio of Steel Frames with Hysteretic Dampers

Jae-Do Kang <sup>1,\*</sup> and Yasuhiro Mori <sup>2</sup>

<sup>1</sup> Earthquake Disaster Mitigation Research Division, National Research Institute for Earth Science and Disaster Resilience, Miki 673-0515, Japan

<sup>2</sup> Graduate School of Environmental Studies, Nagoya University, Nagoya 464-8603, Japan; yasu@sharaku.nuac.nagoya-u.ac.jp

\* Correspondence: kang@bosai.go.jp; Tel.: +81-794-85-8211

Academic Editor: Gangbing Song

Received: 4 March 2017; Accepted: 20 April 2017; Published: 27 April 2017

**Abstract:** In this paper, a simplified method is proposed to estimate the peak inter-story drift ratios of steel frames with hysteretic dampers. The simplified method involved the following: (1) the inelastic spectral displacement is estimated using a single-degree-of-freedom (SDOF) system with multi-springs, which is equivalent to a steel frame with dampers and in which multi-springs represent the hysteretic behavior of dampers; (2) the first inelastic mode vector is estimated using a pattern of story drifts obtained from nonlinear static pushover analysis; and (3) the effects of modes higher than the first mode are estimated by using the  $j$ th modal period,  $j$ th mode vector, and  $j$ th modal damping ratio obtained from eigenvalue analysis. The accuracy of the simplified method is estimated using the results of nonlinear time history analysis (NTHA) on a series of three-story, six-story, and twelve-story steel moment resisting frames with steel hysteretic dampers. Based on the results of a comparison of the peak inter-story drift ratios estimated by the simplified method and that computed via NTHA using an elaborate analytical model, the accuracy of the simplified method is sufficient for evaluating seismic demands.

**Keywords:** simplified estimation method; steel hysteretic damper; peak inter-story drift ratio; inelastic mode vector; equivalent SDOF system

## 1. Introduction

Previous studies conducted over the past two decades have proposed energy dissipation systems that use displacement-dependent dampers and/or velocity-dependent dampers [1]. Currently, a major concern is associated with the need to design a structure with dampers; therefore, many studies have been conducted on this subject [2]. An energy-based design procedure based on achieving a balance between the mean energy dissipated per cycle by a structure and that dissipated by dampers was developed for the seismic retrofitting of existing buildings [3]. By using parameters such as a maximum damper ductility value and an elastic stiffness ratio between the bracing-hysteretic device system and the moment frame system, a design procedure was investigated for frames equipped with a hysteretic energy dissipation device [4,5]. By using a displacement-based design method, a design procedure was investigated for buildings with hysteretic dampers [6–8]. To determine the optimal damper volume related to seismic performance, extant studies have used a performance curve (called as performance spectra) for an elastic system [9,10] and an inelastic system [2,11–13] in the design process of buildings with dampers. However, these studies have not considered the turn from an elastic mode vector to an inelastic mode vector caused by the yielding of a main structure. This would lead to the loss of accuracy

in a large drift range. On the one hand, nonlinear time history analysis (NTHA) using an elaborate analytical model is used to estimate the seismic performance of buildings with dampers. However, this is time-consuming and it is more convenient to perform a seismic performance assessment.

In performance-based seismic design (PBSD), it is essential for the risk associated with the performance level of a structure to be clear and transparent, such that decision makers can understand the expected seismic performance of the structures [14]. Specifically, with respect to PBSD, NTHA using hundreds (or thousands) of ground motion records is required to perform a probabilistic seismic performance assessment of buildings. In recent years, for the seismic performance and probabilistic collapse resistance assessment of buildings with energy dissipation systems, many studies that use incremental dynamic analysis [15] and perform an NTHA using an elaborate analytical model have been conducted [16–20]. However, NTHA using an elaborate analytical model also requires intensive computations to estimate seismic demands [21]. Therefore, a simplified estimation method of inelastic seismic demands is useful, and thus several estimation methods have been proposed by previous studies [22–26]. These methodologies mostly focus on estimating the seismic demands of general buildings and involve the use of equivalent single-degree-of-freedom (SDOF) systems converted from a building structure. In most equivalent SDOF systems, a single skeleton curve is adopted to represent the characteristics of a building structure [24–26]. In order to consider the behavior of dampers, an equivalent SDOF system that includes two springs have been proposed for reinforced concrete buildings with hysteretic dampers by using the results of nonlinear static pushover analysis (NSPA) [27]. However, this model requires interpolation [27], and therefore, the model may necessitate time and effort to approximate the behavior of the springs for the dampers.

In this paper, a simplified method is proposed to estimate the peak inter-story drift ratio of steel frames with hysteretic dampers, and the method is evaluated for use in structural performance assessment. In the method, an equivalent inelastic SDOF system of a steel frame with dampers is presented to estimate the inelastic spectral displacement. The method is also employed to estimate the first inelastic mode vector by using the pattern of story drifts obtained from NSPA. Additionally, in order to consider the effects of modes higher than the first mode, the modal elastic spectral displacement and the participation function are also estimated by using the  $j$ th modal period,  $j$ th mode vector, and  $j$ th modal damping ratio, as obtained from eigenvalue analysis (EVA). In order to estimate the accuracy of the simplified method, the simplified method is compared by using the results of NTHA using an elaborate analytical model on a series of three-story, six-story, and twelve-story steel moment resisting frames with dampers. Parametric analyses are performed for all the frames to confirm the effects of damper properties, such as stiffness and yield deformation, on the accuracy and stability of the simplified method.

## 2. Simplified Method to Estimate the Peak Inter-Story Drift Ratio of Steel Frames with Hysteretic Dampers

In this section, a simplified method is proposed to estimate the inter-story drift ratio of a steel frame with steel hysteretic dampers (called steel metallic dampers), such as buckling-restrained brace dampers and added damping and stiffness dampers. The basic concept employed was presented in a previous study [28]. The method is based on an inelastic modal predictor (IMP) [26], which is an extension of an elastic response spectrum method with a square-root-of-sum-of-squares rule to the inelastic response and is based on extant studies [22,23]. The simplified method also considers the change in the mode vector caused by the yielding of a main building. Additionally, the method accounts for additional steps in the IMP methodology to generate the equivalent SDOF system for estimating the inelastic spectral displacement and for determining the step number  $N$  necessary to derive the inelastic mode vector.

### 2.1. Estimation of Peak Inter-Story Drift Ratios

In this study, based on a previous study [26,28], the peak inter-story drift ratio  $\theta_i^P$  of the  $i$ th story of steel frames with steel hysteretic dampers is evaluated as follows:

$$\theta_i^P = \sqrt{\left(PF_{1,i}^I \cdot Sd_1^I\right)^2 + \sum_{j=2}^n \left(PF_{j,i}^E \cdot Sd_j^E\right)^2} \quad (1)$$

where  $Sd_j^E$  is a  $j$ th modal elastic spectral displacement that is obtained from response spectrum analysis using a  $j$ th modal period and a  $j$ th modal damping ratio obtained from EVA. Additionally,  $PF_{j,i}^E$  denotes the participation function of an inter-story drift ratio for an elastic  $j$ th mode that is defined as follows:

$$PF_{j,i}^E = \frac{\Gamma_j^E \cdot \left({}_s\phi_{j,i}^E - {}_s\phi_{j,i-1}^E\right)}{h_i} \quad (2)$$

where  $h_i$  and  ${}_s\phi_{j,i}^E$  signify the height of the  $i$ th story and the elastic  $j$ th mode vector obtained from EVA of a steel frame with dampers, respectively. In this paper, the subscripts 's' and 'f' before the symbols refer to the entire system and bare frame that is a multi-story frame without dampers, respectively. Furthermore,  $\Gamma_j^E$  denotes the participation factor for the elastic  $j$ th mode that is defined as follows:

$$\Gamma_j^E = \frac{\sum_{i=1}^n m_i \cdot {}_s\phi_{j,i}^E}{\sum_{i=1}^n m_i \cdot \left({}_s\phi_{j,i}^E\right)^2} \quad (3)$$

where  $m_i$  denotes the mass at the  $i$ th story.

In Equation (1),  $Sd_1^I$  implies an inelastic spectral displacement, estimated using the equivalent inelastic SDOF system with multi-springs that is described in Section 2.2. Moreover,  $PF_{1,i}^I$  denotes an inelastic participation function of the inter-story drift ratio evaluated via Equations (2) and (3) with  ${}_s\phi_{j,i}^E$  replaced by  $\phi_i^I$ , which is estimated using the pattern of story drifts obtained from NSPA at the  $N$ th step, corresponding to the  $Sd_1^I$  value obtained from NTHA using the equivalent inelastic SDOF system with multi-springs. The procedure for estimating the inelastic spectral displacement  $Sd_1^I$  and inelastic mode vector  $\phi_i^I$  is explained in Section 2.3.

### 2.2. Equivalent Inelastic SDOF System for Steel Frames with Hysteretic Dampers

This section describes the methodology for converting steel frames with steel hysteretic dampers into an equivalent inelastic SDOF system.

As shown in Figure 1a, the steel hysteretic dampers can be described using shear springs that depend on inter-story drifts. In order to describe an inelastic behavior, a hysteresis rule of a spring in the equivalent SDOF system can be defined by an approximated skeleton curve with respect to a base shear force versus roof drift curve obtained from NSPA, as shown in Figure 1b. When all of the structural components of a building behave in a similar manner, it is possible for an equivalent SDOF system with an assumed single skeleton curve to estimate the inelastic seismic performance of the entire system. However, if the hysteresis rules of each structural member, such as the dampers and frame members, are significantly different, then the assumed single skeleton curve leads to a loss of accuracy in estimating the seismic performance, because the assumed bilinear (or tri-linear) single skeleton curve may not be sufficient to consider the behavior of the dampers.

In the shear frame with dampers (hereafter referred to as the MDOF system), the story shear force is computed by accumulating the lateral force, which is resisted by the column elements and the dampers above the story level. Therefore, the base shear force, which is the shear force on the

first story, is computed by accumulating two lateral forces, namely, the lateral force resisted by the column elements of each story and the lateral force resisted by the dampers of each story. In other words, the lateral force resisted by the dampers can also be divided into several forces, as shown in Figure 1d. Therefore, as shown in Figure 1e, the equivalent SDOF system of the MDOF system can be described using multi-springs with skeleton curves approximated by the base shear force relative to the roof drift curve, as shown in Figure 1d. Based on the fore-mentioned approach, the basic concept of an equivalent inelastic SDOF system with multi-springs was presented in a previous study [28]. Parts of the theoretical development of the method used in this paper are also based on a previous study [28]. The equivalent inelastic SDOF system with multi-springs comprises an effective mass  ${}_s\overline{M}_1$  and an effective height  ${}_s\overline{H}_1$  that are described in Section 2.2.1; an inelastic spring equivalent to the bare frame that is described Section 2.2.2; and inelastic springs equivalent to the dampers that are described Section 2.2.3.

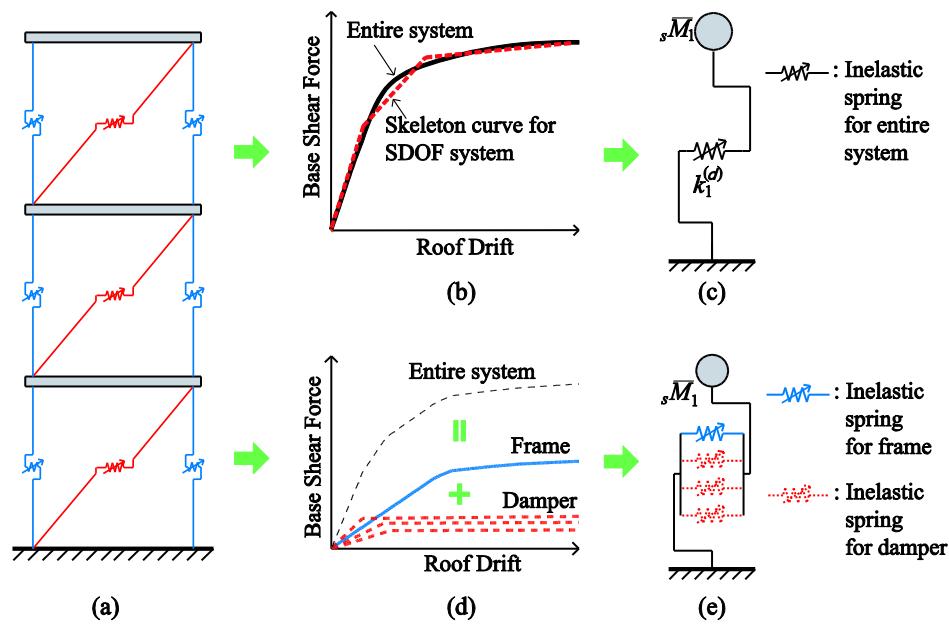


**Figure 1.** A multi-story frame with steel hysteretic dampers: (a) a shear frame with dampers; (b) a single skeleton curve; (c) an equivalent inelastic SDOF system with a single inelastic spring; (d) multi-skeleton curves; and (e) an equivalent inelastic SDOF system with inelastic multi-springs.

### 2.2.1. Mass and Height of Equivalent Inelastic SDOF System

With respect to the first mode, the effective mass  ${}_s\overline{M}_1$  that corresponds to the mass of the equivalent SDOF system, and the effective height  ${}_s\overline{H}_1$  that corresponds to the height of the equivalent SDOF system are expressed, respectively, as follows:

$${}_s\overline{M}_1 = \frac{\left( \sum_{i=1}^n m_i \cdot {}_s\phi_{1,i}^E \right)^2}{\sum_{i=1}^n m_i \cdot {}_s\phi_{1,i}^E} \tag{4}$$

$${}_s\overline{H}_1 = \frac{\sum_{i=1}^n \left( m_i \cdot {}_s\phi_{1,i}^E \cdot H_i \right)}{\sum_{i=1}^n m_i \cdot {}_s\phi_{1,i}^E} \tag{5}$$

where  $n$  and  $H_i$  are the number of stories and the height of the  $i$ th story above the base, respectively.

### 2.2.2. Inelastic Spring Equivalent to Steel Frame

With respect to the first mode, the period  $T_f$  of the bare frame can be obtained from EVA. Additionally, this period is also calculated as follows:

$$T_f = 2\pi \sqrt{\frac{{}_f\overline{M}_1}{k_f}} \tag{6}$$

where  $k_f$  denotes the effective elastic stiffness of the bare frame and  ${}_f\overline{M}_1$  is the effective mass of the bare frame that is defined using Equation (4) with  ${}_s\phi_{1,i}^E$  replaced by  ${}_f\phi_{1,i}^E$ , obtained from EVA of the bare frame.

Equation (6) is used to represent the elastic stiffness  $k_f$  of the bare frame, as follows:

$$k_f = \frac{4 \cdot \pi^2 \cdot {}_f\overline{M}_1}{(T_f)^2} \tag{7}$$

It is assumed that the period calculated by the effective elastic stiffness  ${}_sk_f$  of the spring, which is represented as the only bare frame in the equivalent SDOF system with multi-springs, and the effective mass  ${}_s\overline{M}_1$  is equal to the period of the equivalent SDOF system of the bare frame, as shown in Equation (6). This assumption is represented as follows:

$$T_f = 2\pi \sqrt{\frac{{}_s\overline{M}_1}{{}_sk_f}} = 2\pi \sqrt{\frac{{}_f\overline{M}_1}{k_f}} \tag{8}$$

Based on Equations (7) and (8), the effective elastic stiffness of the spring representing the bare frame in the equivalent SDOF system with multi-springs is defined as follows:

$${}_sk_f = \frac{4 \cdot \pi^2 \cdot {}_s\overline{M}_1}{(T_f)^2} \tag{9}$$

In order to consider the post-elastic behavior of the bare frame, the stiffness reduction factors ( $\gamma_1$  and  $\gamma_2$ ) after the elastic behavior are calculated based on the same method used in a previous study [26], in which a tri-linear skeleton curve is assumed. Further details on the post-yield stiffness can be found in a previous study [26].

The first and second yield drifts on the skeleton curve for the bare frame can be defined as follows:

$$\delta = 1 \frac{\theta_{roof,1} \cdot H_{roof}}{\Gamma_1^E \cdot {}_s\phi_{1,roof}^E}, \quad \delta_2 = \frac{\theta_{roof,2} \cdot H_{roof}}{\Gamma_1^E \cdot {}_s\phi_{1,roof}^E} \tag{10}$$

where  $\theta_{roof,1}$  and  $\theta_{roof,2}$  are the first and second yield drift ratios on the skeleton curve [26], respectively; and  $H_{roof}$  and  ${}_s\phi_{1,roof}^E$  denote the height of the roof above the base and the first mode vector of the roof of the steel frame with dampers, respectively.

The stiffness reduction factors and yield drifts are used to calculate the yield forces  $Q_1$  and  $Q_2$ , as follows:

$$Q_1 = {}_sk_f \cdot \delta_1, \quad Q_2 = {}_sk_f [\delta_1 + \gamma_1(\delta_2 - \delta_1)] \tag{11}$$

Subsequently, the skeleton curve of the inelastic spring that is equivalent to the bare frame is determined by Equations (10) and (11).

### 2.2.3. Inelastic Springs Equivalent to Dampers

This section describes the methodology used to estimate the skeleton curve of the inelastic springs that are equivalent to the dampers in the equivalent SDOF system with multi-springs.

The force versus drift curve of the damper at the  $i$ th story of the MDOF system and the  $i$ th inelastic spring of the equivalent SDOF system are shown in Figure 2a,b, respectively.

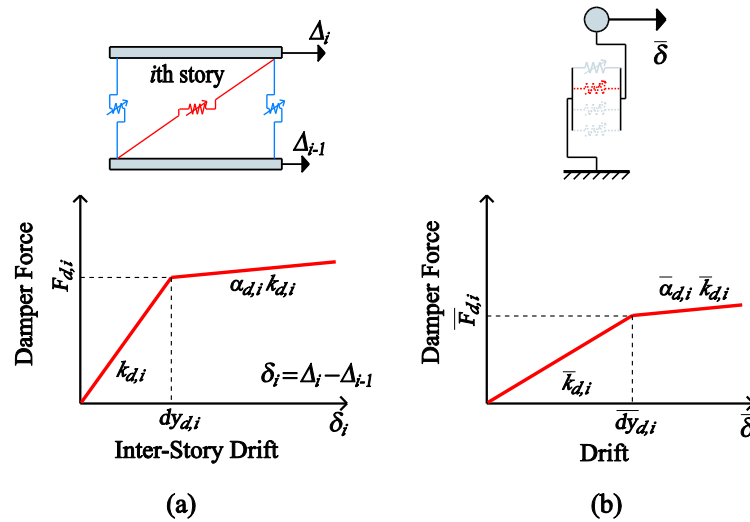


**Figure 2.** Skeleton curves of the dampers and inelastic springs: (a) damper force versus inter-story drift curve of the damper at the  $i$ th story in the MDOF system and (b) force versus drift curve of the  $i$ th spring in the SDOF system.

As shown in the top portion of Figure 2a, by considering only the first mode, a lateral drift  $\Delta_i$  of the  $i$ th story of the MDOF system can be expressed using the drift  $\bar{\delta}$  of the equivalent SDOF system, as shown in the top portion of Figure 2b. This can be expressed as follows:

$$\Delta_i = {}_s\phi_{1,i}^E \cdot \Gamma_1^E \cdot \bar{\delta} \tag{12}$$

where  ${}_s\phi_{1,i}^E$  signifies the first elastic mode vector of the  $i$ th story as obtained from EVA. Thus, the inter-story drift  $\delta_i$  at the  $i$ th story of the MDOF system can be expressed as follows:

$$\delta_i = \Delta_i - \Delta_{i-1} = ({}_s\phi_{1,i}^E - {}_s\phi_{1,i-1}^E) \cdot \Gamma_1^E \cdot \bar{\delta} \tag{13}$$

It is assumed that the energy  $E_{d,i}$  dissipated by the damper at the  $i$ th story of the MDOF system is equivalent to the energy  $\bar{E}_{d,i}$  dissipated by the  $i$ th inelastic spring of the equivalent SDOF system.

Based on this assumption and Equation (13), in the range of  $\delta_i < dy_{d,i}$  that corresponds to the yield deformation of the damper at the  $i$ th story of the MDOF system, the stiffness  $\bar{k}_{d,i}$  of the  $i$ th inelastic spring of the equivalent SDOF system can be expressed as follows:

$$\bar{k}_{d,i} = k_{d,i} ({}_s\phi_{1,i}^E - {}_s\phi_{1,i-1}^E)^2 (\Gamma_1^E)^2 \tag{14}$$

where  $k_{d,i}$  denotes an elastic stiffness of the damper at the  $i$ th story.

Based on a previous assumption that indicates  $E_{d,i} = \bar{E}_{d,i}$  and Equations (13) and (14), when  $\delta_i = dy_{d,i}$ , the yield deformation  $\bar{d}y_{d,i}$  of the  $i$ th inelastic spring of the equivalent SDOF system can be expressed as follows:

$$\bar{d}y_{d,i} = \frac{dy_{d,i}}{({}_s\phi_{1,i}^E - {}_s\phi_{1,i-1}^E) \Gamma_1^E} \tag{15}$$

Based on a previous assumption  $E_{d,i} = \bar{E}_{d,i}$  and Equations (13)–(15), in the range of  $\delta_i > dy_{d,i}$ , a post-elastic stiffness ratio  $\bar{\alpha}_{d,i}$  of the  $i$ th inelastic spring of the equivalent SDOF system can be determined as follows:

$$\bar{\alpha}_{d,i} = \alpha_{d,i} \tag{16}$$

where  $\alpha_{d,i}$  signifies the post-elastic stiffness ratios of the damper at the  $i$ th story.

### 2.3. Procedure for Estimating Inelastic Spectral Displacement and Inelastic Mode Vector

For estimating the peak inter-story drift ratio of the steel frame with steel hysteretic dampers by using Equation (1), the inelastic spectral displacement  $Sd^I$  and the inelastic mode vector  $\phi_i^I$  can be estimated by the following steps (as shown in Figure 3):

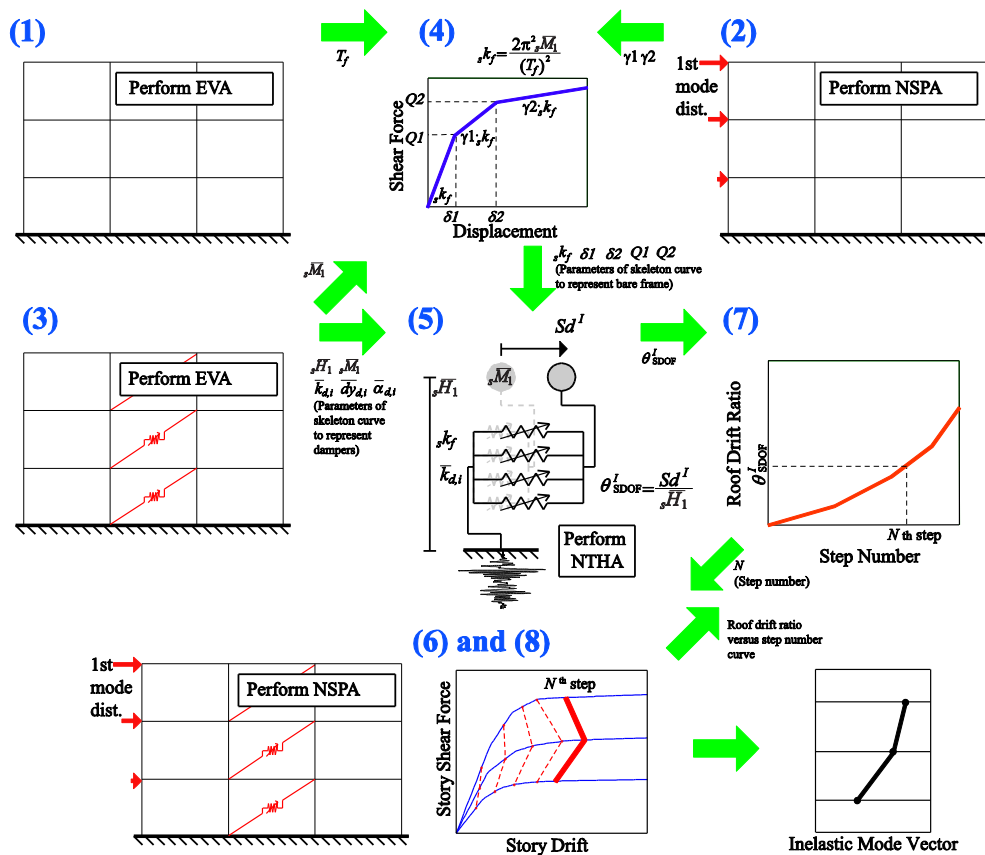


**Figure 3.** Procedure for estimating the inelastic spectral displacement  $Sd^I$  and the inelastic mode vector  $\phi_i^I$ .

- (1) Define the period  $T_f$  for the first mode of the bare frame, as obtained from EVA of the bare frame.
- (2) By using the NSPA results of the bare frame, in which a lateral load pattern is based on the first mode vector, define the stiffness reduction factor to consider the post-elastic behavior of the bare frame.
- (3) Define the mode vector  $s\phi_{1,i}^E$  by performing EVA of the steel frame with dampers. Subsequently, by using Equations (4), (5), and (14)–(16) with  $s\phi_{1,i}^E$ , determine the effective mass  $s\bar{M}_1$ , the effective height  $s\bar{H}_1$ , and the skeleton curves of the inelastic springs equivalent to the dampers.
- (4) By using Equations (9)–(11) with  $s\phi_{1,i}^E$  obtained from Step (3) and the stiffness reduction factor obtained from Step (2), determine the skeleton curve of the inelastic spring equivalent to the bare frame.

- (5) Generate the equivalent inelastic SDOF system with multi-springs using the effective mass  $s\overline{M}_1$ , effective height  $s\overline{H}_1$ , and inelastic springs with the skeleton curves, as obtained from Steps (3) and (4). Subsequently, perform NTHA using the equivalent inelastic SDOF system with multi-springs to evaluate the peak drift ratio, as follows:

$$\theta_{\text{SDOF}}^I = \frac{Sd^I}{s\overline{H}_1} \tag{17}$$

where  $Sd^I$  denotes the inelastic spectral displacement of the steel frame with dampers for the first mode that is obtained from NTHA using an equivalent inelastic SDOF system with multi-springs.

- (6) Obtain the shear force versus the drift curve for each story by performing NSPA of the steel frame with dampers, in which the lateral load pattern is based on the first mode vector.
- (7) Define the step number  $N$  at which the response corresponds to  $\theta_{\text{SDOF}}^I$  in the roof drift ratio versus the step number curve obtained from the NSPA result in Step (6).
- (8) Determine the first inelastic mode vector  $\phi_i^I$  using the pattern of story drifts of the shear force versus the drift curve defined in Step (6) at the  $N$ th step defined in Step (7).

### 3. Numeral Examples

#### 3.1. Building Models

In this paper, a numerical example is considered, as shown in Figure 4, with three two-dimensional steel moment resisting frames (SMRFs) to estimate the accuracy of the simplified method. The SMRFs are designed to satisfy the current seismic requirements in Japan in terms of both strength and drift.

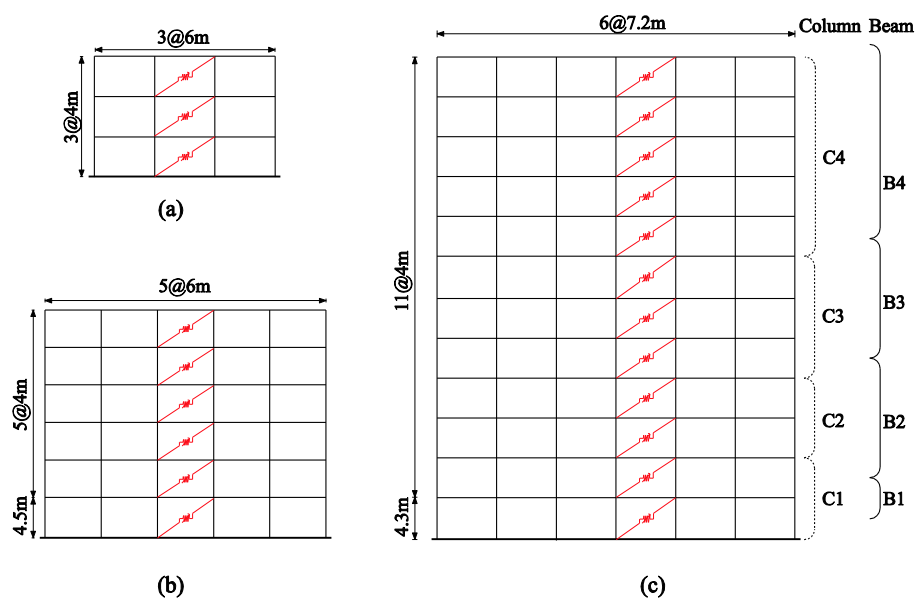


**Figure 4.** Analysis model: (a) a three-story steel moment resisting frame with dampers; (b) a six-story steel moment resisting frame with dampers; and (c) a twelve-story steel moment resisting frame with dampers.

Figure 4a shows the SMRF with three bays of 6.0 m and story heights of 4.0 m. Steel sections of H-350×350×12×19 and H-450×200×9×14 are used for all the columns and all the beams, respectively. The yield strength of the steel material and Young’s modulus are assumed to be 235 N/mm<sup>2</sup> and 205,000 N/mm<sup>2</sup>, respectively. The mass of each story is 70 tons. According to EVA, the fundamental natural period corresponds to 0.758 s. Additionally, NTHA is performed using the nonlinear dynamic

analysis program SNAP ver.7 [29]. In SNAP ver.7, the beams and columns are modeled using the beam element with elasto-plastic characteristics. The nonlinear behaviors of the beams and columns are represented using the concentrated plasticity concept with rotational springs. The rotational behavior of the plastic regions follows a trilinear hysteretic response based on ST3, which is the steel hysteretic material model. The plastic moments at the ends of the columns and beams assume that  $M_p = 592 \text{ kN}\cdot\text{m}$  for the columns and  $M_p = 387 \text{ kN}\cdot\text{m}$  for the beams. The beam and column elements have three degrees of freedom in each node. Tangent stiffness-proportional damping is considered with a 2% damping ratio for the first mode.

Figure 4b shows the SMRF with five bays and six stories. Steel sections of  $\text{H-}400 \times 400 \times 18 \times 28$  and  $\text{H-}500 \times 200 \times 10 \times 16$  are used for all the columns and all the beams, respectively. The yield strength of the steel material is assumed to be  $325 \text{ N/mm}^2$ . The mass of each story is 130 tons. The plastic moments at the ends of the columns and beams assume that  $M_p = 1634 \text{ kN}\cdot\text{m}$  for the columns and  $M_p = 692 \text{ kN}\cdot\text{m}$  for the beams. According to EVA, the fundamental natural period is 1.23 s.

Figure 4c shows the SMRF with six bays and twelve stories. Table 1 also lists the plastic moments at the ends of the columns and beams, and the steel sections. The yield strength of steel is assumed to be  $325 \text{ N/mm}^2$ . The mass of each story is 205 tons. Based on EVA, the fundamental natural period corresponds to 2.17 s.

**Table 1.** Sections and plastic moments of the columns and beams of a twelve-story steel moment resisting frame.

Element	Label	Section	$M_p$ (kN·m)
Columns	C4	□-550×22	2991.7
	C3	□-550×25	3361.7
	C2	□-550×28	3723.0
	C1	□-550×32	4191.2
Beams	B4	H-550×250×12×22	1204.3
	B3	H-550×250×12×25	1322.3
	B2	H-550×250×12×28	1439.0
	B1	H-550×300×14×28	1718.4

### 3.2. Properties of the Hysteretic Dampers

The properties of the steel hysteretic dampers are assumed to be proportional to those of the bare frame. The stiffness ratio  $\kappa$  [10] that corresponds to the ratio of the damper stiffness to the story stiffness of the frame is used to determine the stiffness of the damper at the  $i$ th story, as follows:

$$k_{d,i} = \kappa \cdot k_{f,i} \quad (18)$$

where  $k_{f,i}$  is the lateral story stiffness of the bare frame that is determined by using the NSPA results. The lateral stiffness ratio  $\alpha$  ( $= k_f/k_{total}$  where  $k_{total} = k_f + k_d$ ) of reference [5,13] is equivalent to  $1/(\kappa + 1)$ .

The yield drift ratio  $\nu$  [27] that corresponds to the ratio of the yield deformation of the damper to the story yield drift of the bare frame is used to determine the yield deformation of the damper at the  $i$ th story, as follows:

$$dy_{d,i} = \nu \cdot dy_{f,i} \quad (19)$$

where  $dy_{f,i}$  is the yield story drift of the bare frame that is determined using the NSPA results.

In this paper, the stiffness ratio, the drift ratio, and the post-elastic stiffness ratio of the dampers correspond to two values (1.5 and 3), two values (0.4 and 0.6), and one value (0.03), respectively.

### 3.3. Earthquake Ground Motion Records

In conjunction with the frame models described in the previous section, 73 ground motions selected from the PEER Strong Motion Database are used to investigate the simplified method. A detailed list of the earthquakes can be found in a previous study [22].

### 3.4. Results and Discussion

In this paper, with respect to the simplified method, the first-mode response; first-mode and second-mode responses; and first-mode, second-mode, and third-mode responses are considered for a three-story frame, a six-story frame, and a twelve-story frame with dampers, respectively. In Equation (1), the second and third modal elastic spectral displacements and the participation functions are estimated by using the  $j$ th modal period,  $j$ th mode vector, and  $j$ th modal damping ratio, respectively, as obtained from EVA of the steel frame with dampers.

To confirm the accuracy of the method used to generate an equivalent inelastic SDOF system, the periods obtained from the EVA of the elaborate analytical model are compared with the periods obtained from the EVA of the equivalent SDOF system. According to the comparison results, which are not shown in this paper, the periods of the equivalent SDOF system with multi-springs are equivalent to the periods of an elaborate analytical model.

The accuracy of the simplified method is expressed by the following: (i) its bias denoted as  $a$  that is calculated by the median of the ratio of the peak inter-story drift ratio  $\theta_i^P$ , which is estimated by the simplified method, with respect to the corresponding peak inter-story drift ratio  $\theta_i$ , which is computed via NTHA using the elaborate analytical model; and (ii) its dispersion denoted as  $\sigma$  that is calculated by the standard deviation of the natural logarithms of  $\theta_i^P / \theta_i$ . The parameters bias and the dispersion are equivalently obtained by performing a one-parameter log-log linear least-squares regression of  $\theta_i$  on  $\theta_i^P$ . A bias exceeding unity implies overestimation, while a bias less than unity implies an underestimation of the average by the simplified method. In the paper, the accuracy of the simplified method is confirmed by using 876 results of NTHA using the elaborate analytical model.

The structural demand parameter for evaluation is denoted by the maximum peak inter-story drift ratio  $\theta_{\max}$ , which corresponds to a maximum response over time and a peak with respect to the height of the structure, because  $\theta_{\max}$  correlates well with the structural and nonstructural damage in the structure [30]. Figures 5–7 illustrate the regressions of  $\theta_{\max}$  computed via NTHA using the elaborate analytical model on the  $\theta_{\max}^P$  estimated by the simplified method for a three-story frame, a six-story frame, and a twelve-story frame with dampers, respectively, that are subject to all the earthquake records. The horizontal axis represents the maximum peak inter-story drift ratio that is computed via NTHA using the elaborate analytical model, and the vertical axis corresponds to that estimated by the simplified method. The figures also present the values of bias ( $a$ ) and dispersion ( $\sigma$ ), for which the solid lines and the dotted lines denote the regression lines and the lines of  $\theta_i^P / \theta_i = 1$ , respectively. Based on Figures 5–7, the maximum peak inter-story drift ratios estimated by the simplified method agree fairly well with those computed via NTHA using the elaborate analytical model, irrespective of the difference in the damper parameters with respect to the stiffness ratio  $\kappa$  and the drift ratio  $v$ . The biases and dispersions of the simplified method are in the range of 0.995–1.01 and 0.041–0.053, respectively, for the three-story frame, as shown in Figure 5; 0.992–1.012 and 0.051–0.075, respectively, for the six-story frame, as shown in Figure 6; and 1.005–1.033 and 0.059–0.075, respectively, for the twelve-story frame, as shown in Figure 7. The ranges of the bias and dispersion of the simplified method increase as the height of the structure increases. However, the value does not affect the estimation of the accuracy of the simplified method because the increase in the value is very small.

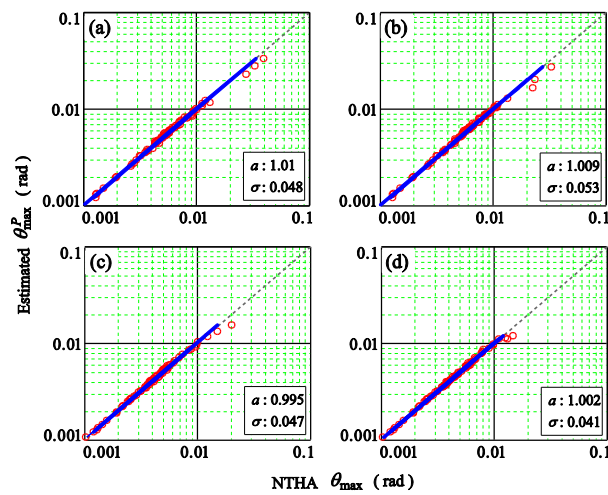


Figure 5. Regressions of  $\theta_{\max}$  on  $\theta_{\max}^P$  for a three-story frame with dampers: (a)  $\kappa = 1.5$  and  $\nu = 0.4$ ; (b)  $\kappa = 1.5$  and  $\nu = 0.6$ ; (c)  $\kappa = 3$  and  $\nu = 0.4$ ; and (d)  $\kappa = 3$  and  $\nu = 0.6$ .

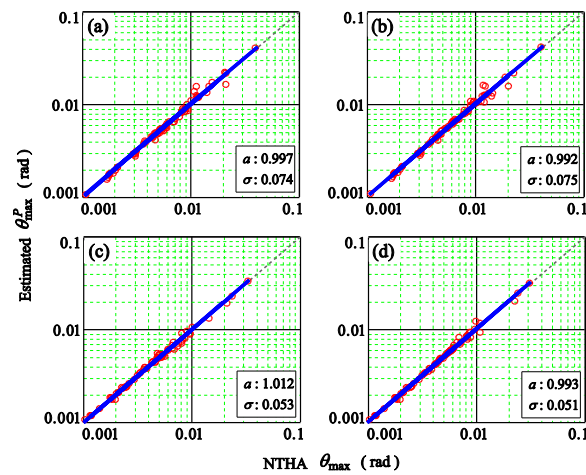


Figure 6. Regressions of  $\theta_{\max}$  on  $\theta_{\max}^P$  for a six-story frame with dampers: (a)  $\kappa = 1.5$  and  $\nu = 0.4$ ; (b)  $\kappa = 1.5$  and  $\nu = 0.6$ ; (c)  $\kappa = 3$  and  $\nu = 0.4$ ; and (d)  $\kappa = 3$  and  $\nu = 0.6$ .

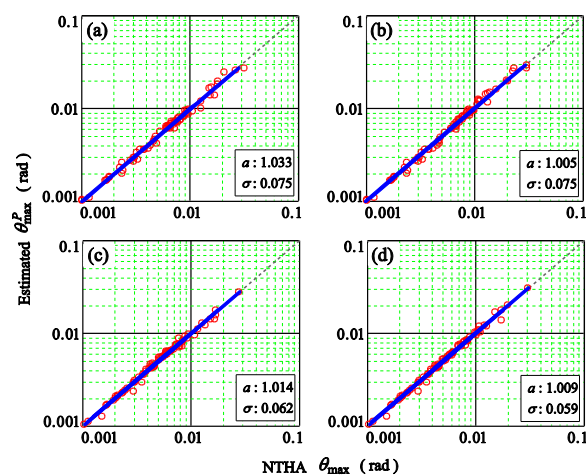
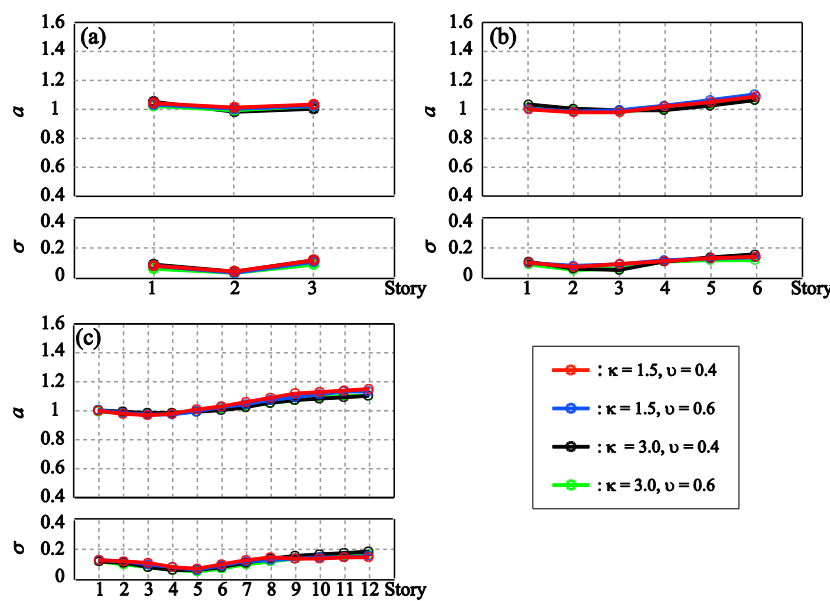


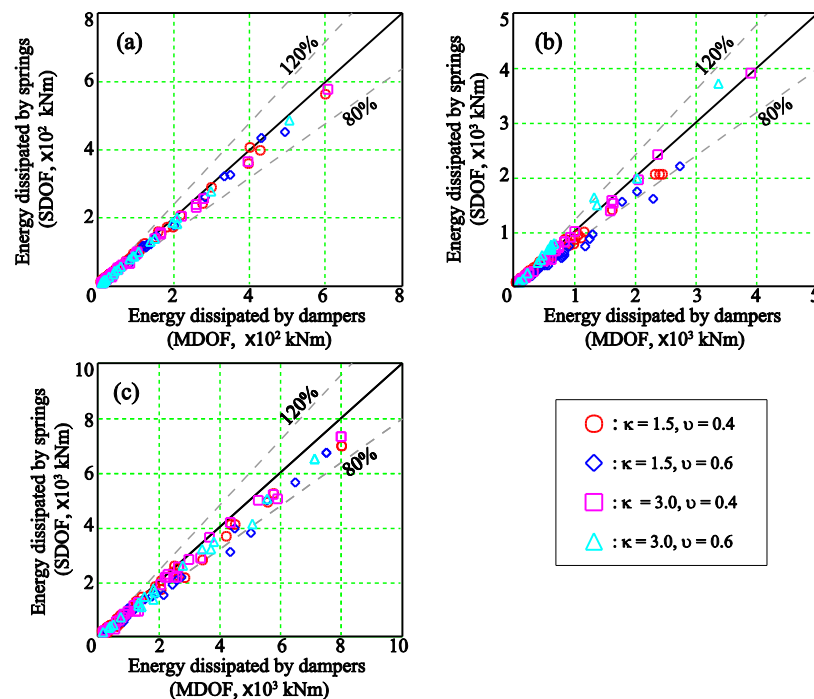
Figure 7. Regressions of  $\theta_{\max}$  on  $\theta_{\max}^P$  for a twelve-story frame with dampers: (a)  $\kappa = 1.5$  and  $\nu = 0.4$ ; (b)  $\kappa = 1.5$  and  $\nu = 0.6$ ; (c)  $\kappa = 3$  and  $\nu = 0.4$ ; and (d)  $\kappa = 3$  and  $\nu = 0.6$ .

Figure 8 summarizes the bias ( $a$ ) and the dispersion ( $\sigma$ ) of the simplified method for: (a) a three-story frame; (b) a six-story frame; and (c) a twelve-story frame with dampers that are subjected to all the earthquake records. The biases and dispersions of  $\theta_i^P$  estimated by the simplified method are in the range of 0.972–1.151 and 0.025–0.179, respectively, for all the frames. In the case where  $\kappa = 1.5$ , as shown in Figure 8c, the biases of  $\theta_i^P$  estimated by the simplified method exceed 1.1 for the upper stories (i.e., 9–12 stories) of the twelve-story frame with dampers. However, the biases of  $\theta_i^P$  for the other stories of all the frames are less than 1.1. Additionally, the dispersions of  $\theta_i^P$  estimated by the simplified method are less than 0.02 for all the stories of all the frames. Therefore, the accuracy of the simplified method is sufficient for evaluating the seismic demands, irrespective of the difference in the damper parameters.

In this paper, the assumption  $E_{d,i} = \bar{E}_{d,i}$  is used to convert the steel frame with dampers into an equivalent SDOF system. To confirm this assumption, Figure 9 shows a one-to-one comparison between the total energy dissipated by the dampers in the elaborate analytical model and the total energy dissipated by the inelastic springs in the equivalent SDOF system. The vertical axis represents the total energy dissipated by the springs of the equivalent SDOF system, and the horizontal axis signifies the total energy dissipated by the dampers of the elaborate analytical model. As shown in Figure 9a, the total energies dissipated by the springs agree well with those dissipated by the dampers. In contrast, the total energy dissipated by the springs fluctuates slightly when compared with the total energy dissipated by the dampers, as shown in Figure 9b,c. However, the total energy dissipated by the springs agrees well with the total energy dissipated by the dampers, irrespective of the difference in the magnitude of an earthquake. Therefore, the accuracy of the equivalent SDOF system is sufficient to evaluate the seismic demands, irrespective of the difference in the damper parameters with respect to the stiffness ratio  $\kappa$  and the drift ratio  $v$ .



**Figure 8.** Bias ( $a$ ) and dispersion ( $\sigma$ ) of the simplified method: (a) for a three-story frame with dampers; (b) for a six-story frame with dampers; and (c) for a twelve-story frame with dampers.



**Figure 9.** One-to-one comparison between energy dissipated by dampers in an elaborate analytical model and energy dissipated by springs in an equivalent inelastic SDOF system: (a) for a three-story frame with dampers; (b) for a six-story frame with dampers; and (c) for a twelve-story frame with dampers.

#### 4. Conclusions

In this paper, a simplified method is proposed to estimate the peak inter-story drift ratio of steel multi-story frames with steel hysteretic dampers. In this method, with respect to the first mode, the inelastic spectral displacement of a steel frame with dampers is estimated by using an equivalent inelastic SDOF system that includes multi-springs in order to consider the hysteretic behavior of dampers, and the inelastic mode vector is estimated by using a pattern of story drifts that is obtained from NSPA of a steel frame with dampers with a lateral load pattern based on the first mode vector. Additionally, in order to consider the effects of modes higher than the first mode, the second and third modal elastic spectral displacement and the participation functions are also estimated by using the  $j$ th modal period,  $j$ th mode vector, and  $j$ th modal damping ratio, respectively, as obtained from EVA of the steel frame with dampers. In order to estimate the accuracy of the simplified method, the simplified method is compared by using the results of NTHA that use an elaborate analytical model on a series of three-story, six-story, and twelve-story SMRFs with dampers. In order to confirm the effects of the damper properties, such as stiffness and yield deformation, on the accuracy and stability of the simplified method, parametric analyses are performed for all the frames that are subjected to all the earthquake records. The results indicate that the accuracy of the simplified method is sufficient to evaluate the seismic demands, irrespective of the difference in damper parameters. Therefore, this method reduces the computational time and effort required to perform a seismic performance assessment.

Further, studies on different structural buildings such as a reinforced concrete structures and studies on different layouts of dampers are needed to gain more insight into the efficiency of the proposed method.

**Acknowledgments:** This work was supported by Grant-in-Aid for JSPS Fellows (No. 26.7166).

**Author Contributions:** Jae-Do Kang designed this work, conducted all the analytical work, and wrote the manuscript. Yasuhiro Mori supervised and reviewed this work.

**Conflicts of Interest:** The authors declare no conflict of interest.

## References

1. Symans, M.; Charney, F.; Whittaker, A.; Constantinou, M.; Kircher, C.; Johnson, M.; McNamara, R. Energy dissipation systems for seismic applications: Current practice and recent developments. *J. Struct. Eng.* **2008**, *134*, 3–21. [[CrossRef](#)]
2. Pu, W.; Liu, C.; Zhang, H.; Kasai, K. Seismic control design for slip hysteretic timber structures based on tuning the equivalent stiffness. *Eng. Struct.* **2016**, *128*, 199–214. [[CrossRef](#)]
3. Benavent-Climent, A. An energy-based method for seismic retrofit of existing frames using hysteretic dampers. *Soil Dyn. Earthq. Eng.* **2011**, *31*, 1385–1396. [[CrossRef](#)]
4. Vargas, R.; Bruneau, M. Analytical response and design of buildings with metallic structural fuses. I. *J. Struct. Eng.* **2009**, *135*, 386–393. [[CrossRef](#)]
5. Tena-Colunga, A.; Nangullasmú-Hernández, H. Assessment of seismic design parameters of moment resisting RC braced frames with metallic fuses. *Eng. Struct.* **2015**, *95*, 138–153. [[CrossRef](#)]
6. Lin, Y.-Y.; Tsai, M.; Hwang, J.; Chang, K. Direct displacement-based design for building with passive energy dissipation systems. *Eng. Struct.* **2003**, *25*, 25–37. [[CrossRef](#)]
7. Kim, J.; Seo, Y. Seismic design of low-rise steel frames with buckling-restrained braces. *Eng. Struct.* **2004**, *26*, 543–551. [[CrossRef](#)]
8. Martínez, C.A.; Curadelli, O.; Compagnoni, M.E. Optimal placement of nonlinear hysteretic dampers on planar structures under seismic excitation. *Eng. Struct.* **2014**, *65*, 89–98. [[CrossRef](#)]
9. Kasai, K.; Fu, Y.; Watanabe, A. Passive control systems for seismic damage mitigation. *J. Struct. Eng.* **1998**, *124*, 501–512. [[CrossRef](#)]
10. Japan Society of Seismic Isolation. *Design and Construction Manual for Passively Controlled Buildings*, 2nd ed.; Japan Society of Seismic Isolation (JSSI): Tokyo, Japan, 2005.
11. Kasai, K.; Pu, W. Passive control design method for MDOF slip-hysteretic structure added with visco-elastic damper. *J. Struct. Constr. Eng.* **2010**, *75*, 781–790. [[CrossRef](#)]
12. Kasai, K.; Ogawa, R.; Pu, W.; Kiyokawa, T. Passive control design method for elasto-plastic frame added with visco-elastic dampers. *J. Struct. Constr. Eng.* **2010**, *75*, 1625–1633. [[CrossRef](#)]
13. Guo, J.W.W.; Christopoulos, C. Performance spectra based method for the seismic design of structures equipped with passive supplemental damping systems. *Earthq. Eng. Struct. Dyn.* **2013**, *42*, 935–952. [[CrossRef](#)]
14. Xue, Q.; Chen, C.C. Performance-based seismic design of structures: A direct displacement-based approach. *Eng. Struct.* **2003**, *25*, 1803–1813. [[CrossRef](#)]
15. Vamvatsikos, D.; Cornell, C.A. Incremental dynamic analysis. *Earthq. Eng. Struct. Dyn.* **2002**, *31*, 491–514. [[CrossRef](#)]
16. Seo, C.Y.; Karavasilis, T.L.; Ricles, J.M.; Sause, R. Seismic performance and probabilistic collapse resistance assessment of steel moment resisting frames with fluid viscous dampers. *Earthq. Eng. Struct. Dyn.* **2014**, *43*, 2135–2154. [[CrossRef](#)]
17. Silwal, B.; Ozbulut, O.E.; Michael, R.J. Seismic collapse evaluation of steel moment resisting frames with superelastic viscous damper. *J. Constr. Steel Res.* **2016**, *126*, 26–36. [[CrossRef](#)]
18. Karavasilis, T.L. Assessment of capacity design of columns in steel moment resisting frames with viscous dampers. *Soil Dyn. Earthq. Eng.* **2016**, *88*, 215–222. [[CrossRef](#)]
19. Dimopoulos, A.I.; Tzimas, A.S.; Karavasilis, T.L.; Vamvatsikos, D. Probabilistic economic seismic loss estimation in steel buildings using post-tensioned moment-resisting frames and viscous dampers. *Earthq. Eng. Struct. Dyn.* **2016**, *45*, 1725–1741. [[CrossRef](#)]
20. Kim, J.; Shin, H. Seismic loss assessment of a structure retrofitted with slit-friction hybrid dampers. *Eng. Struct.* **2017**, *130*, 336–350. [[CrossRef](#)]

21. Luco, N.; Mori, Y.; Funahashi, Y.; Cornell, C.A.; Nakashima, M. Evaluation of predictors of non-linear seismic demands using ‘fishbone’ models of SMRF buildings. *Earthq. Eng. Struct. Dyn.* **2003**, *32*, 2267–2288. [[CrossRef](#)]
22. Luco, N. Probabilistic Demand Analysis, SMRF Connection Fractures, and Near-Source Effects. Ph.D. Thesis, Stanford University, Stanford, CA, USA, 2002.
23. Luco, N.; Cornell, C.A. Structure-specific scalar intensity measures for near-source and ordinary earthquake ground motions. *Earthq. Spectra* **2007**, *23*, 357–392. [[CrossRef](#)]
24. Kuramoto, H.; Teshigawara, M.; Okuzono, T.; Koshika, N.; Takayama, M.; Hori, T. Predicting the earthquake response of buildings using equivalent single degree of freedom system. In Proceedings of the 12th World Conference on Earthquake Engineering, Auckland, New Zealand, 30 January–4 February 2000; No. 1039.
25. Chopra, A.K.; Goel, R.K. A modal pushover analysis procedure for estimating seismic demands for buildings. *Earthq. Eng. Struct. Dyn.* **2002**, *31*, 561–582. [[CrossRef](#)]
26. Mori, Y.; Yamanaka, T.; Luco, N.; Cornell, C.A. A static predictor of seismic demand on frames based on a post-elastic deflected shape. *Earthq. Eng. Struct. Dyn.* **2006**, *35*, 1295–1318. [[CrossRef](#)]
27. Oviedo, J.A.; Midorikawa, M.; Asari, T. An equivalent SDOF system model for estimating the response of R/C building structures with proportional hysteretic dampers subjected to earthquake motions. *Earthq. Eng. Struct. Dyn.* **2011**, *40*, 571–589. [[CrossRef](#)]
28. Kang, J.-D.; Mori, Y. Simplified method for estimating inelastic seismic demand of multistory frame with displacement-dependent passive dampers. In Proceedings of the 5th Asia Conference on Earthquake Engineering, Taipei, Taiwan, 16–18 October 2014; No. 149.
29. *SNAP Technical Manual*, 7th ed.; Kozo System, Inc.: Tokyo, Japan, 2015.
30. Tothong, P.; Cornell, C.A. Structural performance assessment under near-source pulse-like ground motions using advanced ground motion intensity measures. *Earthq. Eng. Struct. Dyn.* **2008**, *37*, 1013–1037. [[CrossRef](#)]



© 2017 by the authors. Licensee MDPI, Basel, Switzerland. This article is an open access article distributed under the terms and conditions of the Creative Commons Attribution (CC BY) license (<http://creativecommons.org/licenses/by/4.0/>).